

# QUENCH AND MECHANICAL PERFORMANCE OF 1-M MODEL MAGNETS FOR THE LHC LOW BETA QUADRUPOLES

T. Nakamoto, T. Ogitsu, Y. Ajima, E. Burkhardt, N. Higashi, H. Hirano,  
M. Iida, N. Kimura, H. Ohhata, N. Ohuchi, T. Shintomi, K. Sugita, K. Tanaka,  
A. Terashima, K. Tsuchiya, A. Yamamoto, KEK, Tsukuba, Japan  
S. Murai, O. Oosaki, T. Orikasa, Toshiba, Yokohama, Japan

## Abstract

Two 1-m model magnets for the LHC low-beta insertion quadrupole have been developed. One was fabricated by KEK to confirm the magnet performance with the final cross section. Another model that was identically designed was built at Toshiba to confirm the technical transfer. In the curing process, the coil size was controlled by the optimised curing shim thickness. These magnets were connected in series and simultaneously tested at 1.9 K. Quench history of the present models showed better performance than the previous model and the magnets were verified to reach the LHC operational current without a quench after a thermal cycle. The R&D phase of the LHC insertion quadrupole will move to development of 6-m long prototype.

## 1 INTRODUCTION

Development of 70 mm aperture superconducting quadrupole magnets for the LHC low-beta insertion, so called as MQXA, is under way at KEK. The development is a part of the collaboration between KEK and CERN for the LHC, and sixteen 6-m long magnets will be installed in low-beta beam insertion regions of the LHC together with other 16 magnets by FNAL.

After the R&D of the two 1-m long model magnets, the third 1-m model (Model #03) was fabricated with a new coil design and the magnet performance was tested [1]. The fourth model (Model #04) was produced so that the quench performance and the field quality were compared with model #03. The fifth, identically designed, model magnet (Model #05) was built at Toshiba Keihin Product, that is the fabricator of the 6-m long prototypes and the production magnets, to confirm the technical transfer from KEK to the company. These magnets were tested at KEK with a new vertical cryostat [2] made for the 6-m long production magnet. To compromise with the test schedule, the magnets were connected in series and excited simultaneously. This paper reports the quench performance and the mechanical behavior of models #04 and #05. Detailed report on the field quality is separately presented at this conference [3].

## 2 DESIGN AND FABRICATION

Main design parameters of the new magnets are listed in Table 1, and progress of the design study and R&D works have been reported in [4]-[7].

Table 1: Main design parameters of low-beta insertion quadrupoles for LHC

|                            |  | Models #04 and #05          |
|----------------------------|--|-----------------------------|
| Field Gradient (T/m)       |  |                             |
| Design (Operation)         |  | 240 (215)                   |
| Current (A)                |  |                             |
| Design (Operation)         |  | 8057 (7150)                 |
| Peak Field (T)             |  | 9.62                        |
| Load Line Ratio (%)        |  |                             |
| Inner Cable; IC            |  | 91                          |
| Outer Cable; OC            |  | 88                          |
| Number of Turns per Pole   |  |                             |
| 1st Layer Coil             |  | 8 (IC)+4 (IC)<br>with wedge |
| 2nd Layer Coil             |  | 12(OC)+4 (IC)<br>with wedge |
| 3rd Layer Coil             |  | 15 (OC)                     |
| 4th Layer Coil             |  | 18 (OC)                     |
| Stored Energy (kJ/m)       |  | 442                         |
| Inductance (mH/m)          |  | 13.6                        |
| Magnetic Forces per Octant |  |                             |
| F <sub>x</sub> (MN/m)      |  | 1.45                        |
| F <sub>y</sub> (MN/m)      |  | -1.72                       |

Table 2: Relative coil thickness and Young's modulus of inner- and outer- coils at 50 MPa

| Magnet    | Relative coil thickness ( $\mu\text{m}$ ) |            | Young's modulus (GPa) |            |
|-----------|---|------------|-----------------------|------------|
|           | Inner coil                                | Outer coil | Inner coil            | Outer coil |
| Model #03 | 89 (16)                                   | 145 (28)   | 6.5 (0.2)             | 7.1 (0.3)  |
| Model #04 | 33 (18)                                   | 100 (19)   | 8.4 (0.3)             | 8.1 (0.4)  |
| Model #05 | 4 (13)                                    | 9 (15)     | 7.5 (0.2)             | 9.2 (0.6)  |

Inner coil: 1st and 2nd layers, Outer coil: 3rd and 4th layers.

Numbers in parenthesis indicate statistical errors ( $1\sigma$ ).

Models #03, #04 and #05 were identically designed and fabricated except for the curing process: different shim thickness was adopted to each magnet to adjust the coil size. Table 2 summarizes the relative coil thickness to the original design value and the Young's modulus of the first- and the second- layer (inner) coils and the third- and the fourth layer (outer) coils. Numbers in parenthesis indicate statistical errors ( $1\sigma$ ). The mechanical measurement was performed right after the first curing process: each inner and outer coil was separately cured. By choosing the appropriate shim thickness, the coil size gradually approached to the design value. Smaller coil

thickness generally traded off the higher Young's modulus. Both of the thickness and the Young's modulus of models #04 and #05 distributed within small deviation and the median plane shift was expected to be small enough.

Figure 1 plots the relative coil thickness and the Young's modulus of the 4-layer coils as a function of the stress. The measurement was made right after the second curing process that gathered the inner- and the outer- coils to be the 4-layer coil. The left hand vertical axis is the relative thickness to the original design value which the pre-stress of 50 MPa will be obtained after the magnet assembly. Error bars indicate statistical errors ( $1\sigma$ ). As shown in the figure, each coil size was shifted and controlled in all stress range by varying the shim thickness. Model #05 was cured to be about 150  $\mu\text{m}$  smaller than model #03 and the coil size was fairly adjusted to the original design value at 50 MPa.

Table 3 lists the azimuthal coil pre-stress during the magnet assembly. The pre-stress was determined by the capacitive transducers installed between the coil and the stainless collar. Although the thickness of models #04 and #05 became smaller, the pre-stresses were almost same as model #03. This might be due to the dimensional problem of the brass shoes where the transducers were mounted. The unbalance of the pre-stress between the inner- and the outer- coils was reduced in model #05 by adjusting the coil size.

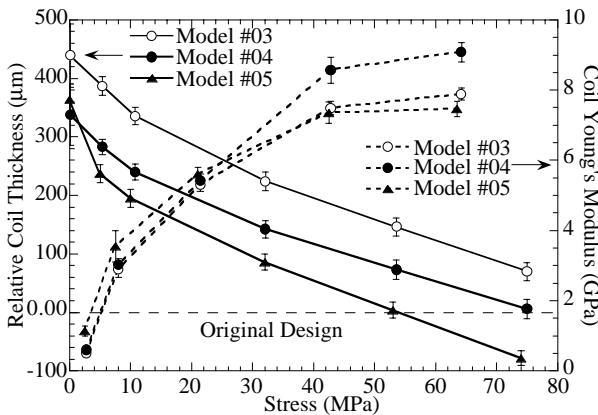


Figure 1: Relative coil thickness and Young's modulus of 4-layer coils. Bars indicate statistical errors ( $1\sigma$ ).

Table 3: Azimuthal coil pre-stress during assembly process (MPa)

| Process   | #03   |       | #04   |       | #05   |       |
|-----------|-------|-------|-------|-------|-------|-------|
|           | Inner | Outer | Inner | Outer | Inner | Outer |
| Collaring | <5    | <5    | <5    | <5    | <5    | <5    |
| Yoking    | 40    | 53    | 37    | 58    | 41    | 47    |

### 3 EXCITATION TESTS

#### 3.1 Quench History

Models #04 and #05 were simultaneously excited at 1.9 K with a ramp-rate of 10 A/sec in series connection, and approximately half of the stored energy was extracted from

the magnet by using a 50 m $\Omega$  dump resistor with firing the quench protection heaters (QPHs). The excitation tests were performed in the vertical cryostat newly constructed for the 6-m long production magnets. A 3-m long stainless steel cylindrical vacuum chamber was suspended below the model magnets as a dummy void so that the amount of superfluid helium coolant was saved and the cool-down time was minimized. The both models experienced a full thermal cycle to room temperature to observe the training memory. Further quench studies such as fast ramp tests, AC loss tests, temperature dependence tests or heater tests were not performed on these magnets.

Quench history of models #04 and #05 is shown in Fig. 2. The first quench occurred at 7326 A which exceeded the LHC operational current of 7150 A ( $G=215$  T/m). The following quench currents went up rapidly and the magnets only needed four quenches to reach the field gradient of 230 T/m: a guide line to judge the quench performance of MQXA at the magnet test in KEK. After reaching to 230 T/m, however, the quench curve seemed to be saturated.

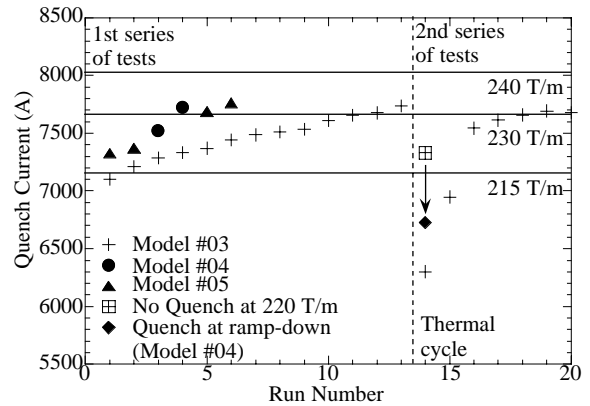


Figure 2: Quench history of models #04 and #05.

After the first series of tests, the magnets experienced a thermal cycle to room temperature. Since a technical problem took place with the power supply, the series of quench tests were stopped. The magnets were once energized up to the field gradient of 220 T/m to prove the training memory after the thermal cycle. The magnets, as shown in Fig. 2, successfully reached to 220 T/m ( $I=7330$  A) without a quench although they quenched during the following ramp-down process. This unexpected quench was not understood.

Table 4 lists the quench locations of models #04 and #05. Quench locations could not be precisely localized due to the lack of digitizers for the voltage taps and the quenched layer-coils are only listed in this table. According to this table, the quench locations were distributed in all poles, but concentrated in the second layer coils. Recent training results of the first 6-m prototype also indicated that the most quenches initiated in the second layer coils. It can be concluded that the MQXA designed magnets have weak regions in the second

layer coils except for model #03 which mostly quenched in the fourth layer coils possibly due to the misalignment of the insulating films.

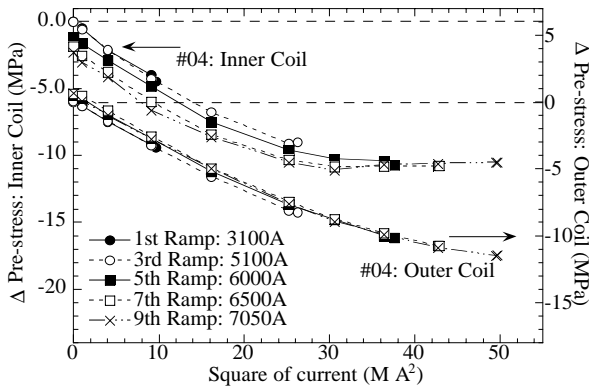
Table 4: Quench locations of models #04 and #05.

| Quench Number | Quench Current (A) | MIITs (MA <sup>2</sup> s) | Quench Location       |
|---------------|--------------------|---------------------------|-----------------------|
| 1st test      | 1                  | 7326                      | #05, Pole2, 2nd layer |
|               | 2                  | 7369                      | #05, Pole3, 2nd layer |
|               | 3                  | 7520                      | #04, Pole4, 2nd layer |
|               | 4                  | 7725                      | #04, Pole2, 2nd layer |
|               | 5                  | 7688                      | #05, Pole3, 2nd layer |
|               | 6                  | 7763                      | #05, Pole4, 2nd layer |
| 2nd test      | 7                  | 6725                      | #04, Pole3, 2nd layer |

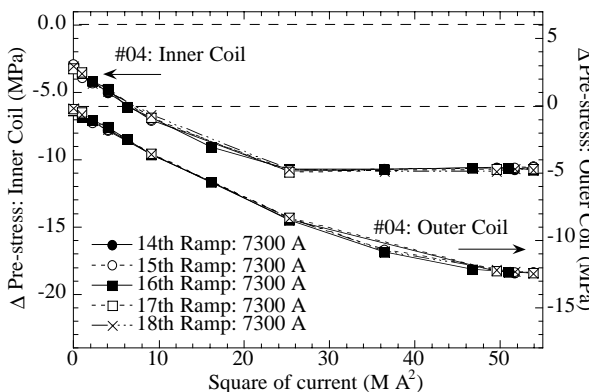
### 3.2 Mechanical Behaviour during Excitation

Figures 3(a) and (b) show azimuthal pre-stress change of model #04 during excitation before and after the first training quench, respectively. Pre-stress changes were plotted as a function of square of the current and normalized to be zero at the initial pre-stress right after the cool-down.

In Fig. 3(a), the pre-stress curves of the inner coil were gradually shifted to lower values as the magnet was repeatedly energized with increasing the ramp-up current



(a)



(b)

Figure 3: Azimuthal pre-stress change of model #04 during excitation (a) before and (b) after first training quench.

before the first training quench. The curves became stabilised after the seventh excitation up to 6500 A, and the pre-stress was about 3 MPa lower than the initial value right after the cool-down. The pre-stress changes after the first quench in Fig. 3(b) precisely trace this curve. The pre-stress change curves were saturated at the current region above 5000 A. The lower pre-stress of the inner coil, however, did not affect the training characteristics because the first quench took place over 7300 A and the training successfully went on.

For the outer coil, the pre-stress curves were distributed within 1 MPa and decreased linearly: no saturation was observed. These mechanical behaviours were consistently observed in model #05.

## 4 SUMMARY AND FURTHER PLAN

Models #04 and #05 exceeded the operational field gradient of 215 T/m without a quench and reached to 230T/m after 4 quenches. The acceptable training memory after the full thermal cycle was confirmed.

The R&D program of 1-m model magnets for the LHC-MQXA was completed. The 6-m long prototype was fabricated at Toshiba and the excitation test is in progress at KEK.

## REFERENCES

- [1] T. Nakamoto et al., "Quench performance and mechanical behavior of 1 m model magnet for the LHC low-beta quadrupoles at KEK," to be published as Proc. ASC2000 in IEEE Appl. Super.
- [2] N. Kimura et al., "A pressurized HeII cryogenics system for the superconducting magnet test facility at KEK," to be presented at CEC/ICMC 2001, C-01D-05.
- [3] N. Ohuchi et al., "Field quality of the LHC-IRQ 1-m model quadrupole magnets developed at KEK," to be presented at this conference, P2hc02.
- [4] A. Yamamoto et al., "Design study of a superconducting insertion quadrupole magnet for the Large Hadron Collider," IEEE Appl. Super., vol. 7, no. 2, pp. 747-750, 1997.
- [5] A. Yamamoto et al., "Development of a superconducting insertion quadrupole magnet for the Large Hadron Collider," Proc. 15th Inter. Conf. Magn. Tech., pp. 59-62, 1998.
- [6] G. A. Kirby et al., "Mechanical design and characteristics of a superconducting insertion quadrupole model magnet for the Large Hadron Collider," Proc. 15th Inter. Conf. Magn. Tech., pp. 63-66, 1998.
- [7] K. Tsuchiya et al., "Magnetic design of a low-beta quadrupole magnet for the LHC insertion regions," IEEE Appl. Super., vol. 10, No. 1, 135-138, 2000.